

# Synthesis by Direct Arylation of Thiazole–Derivatives: Regioisomer Configurations–Optical Properties Relationship Investigation

Patricia Chávez,<sup>†</sup> Chheng Ngov,<sup>†</sup> Pierre de Frémont,<sup>‡</sup> Patrick Lévêque,<sup>\*,§</sup> and Nicolas Leclerc<sup>\*,†</sup>

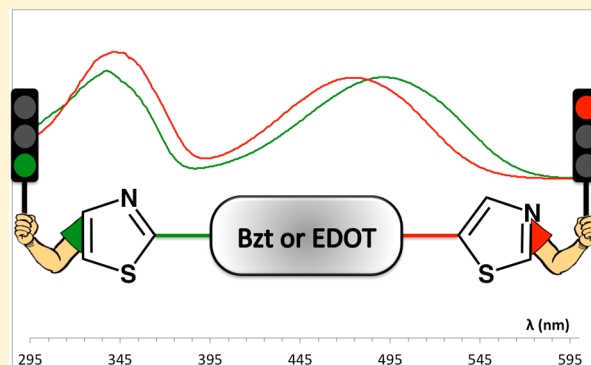
<sup>†</sup>Institut de Chimie et Procédés pour l'Energie, l'Environnement et la Santé (ICPEES), Département d'Ingénierie Polymère, UMR 7515 au CNRS, Ecole Européenne de Chimie, Polymères et Matériaux, 25 rue Becquerel, 67087 Strasbourg Cedex 02, France

<sup>‡</sup>Laboratoire de Chimie de Coordination, Institut de Chimie, UMR 7177-CNRS, Université de Strasbourg, 4 rue Blaise Pascal, 67070 Strasbourg, France

<sup>§</sup>Laboratoire des Sciences de l'Ingénieur, de l'Informatique et de l'Imagerie (ICube), UMR 7357 Université de Strasbourg-CNRS, 23 rue du Loess, 67037 Strasbourg Cedex 02, France

## Supporting Information

**ABSTRACT:** The synthesis of thiazole(Tz)-based regioisomer materials using selective direct arylation to avoid any protection steps has been developed. A series of trimers in which the Tz groups sandwich either an electron-rich or an electron-deficient unit, with a regioselective orientation of the respective Tz unit, has therefore been synthesized. This chemical strategy has also been followed to synthesize a second series of pentamers in which the Tz group is used as a  $\pi$ -conjugated bridge between an electron-rich central unit and electron-deficient end-capping groups and vice versa. On both trimers and pentamers, the effect of Tz orientation on the conjugation properties of the synthesized materials was investigated by a combination of experimental measurements and density functional theory calculations. This study highlights that control of the orientation of the Tz unit leads to the synthesis of the most conjugated regioisomer derivative. The present work gives chemical synthesis tools for the synthesis of selectively oriented Tz-based materials as well as a general guideline for the design of Tz-based materials with the highest conjugation length, including the Tz-orientation effect.



## INTRODUCTION

In the field of organic materials presenting a high nonlinear optical (NLO) response, thiazole (Tz) (Figure 1, left) has attracted a lot of interest.<sup>1</sup> Usually, an organic NLO compound is composed of electron-rich and electron-poor moieties bridged by a  $\pi$ -conjugated linker.<sup>2</sup> The alternation of electron-rich (D) and electron-deficient (A) moieties bridged by a  $\pi$ -conjugated linker is also widely used to design low-band-gap copolymers in the field of organic photovoltaic (OPV) devices. However, the use of Tz units as a building block for OPV materials is not well referenced. Most OPV literature data are related to the use of thiazolothiazole,<sup>3</sup> 5,5'-bithiazole<sup>4</sup>, and bridged-bithiazole<sup>5</sup> as electron-deficient building blocks rather than as single Tz units. Recently, we suggested that Tz could be used as a weak electron-acceptor group as well as a weak electron-donor group, depending on the neighboring substituted chemical unit in the OPV-conjugated molecules.<sup>6</sup> In the present study, we investigate the effect of Tz-unit orientation on the optoelectronic properties of OPV D/A-alternating compounds when Tz is directly used as an electron-rich or electron-deficient unit or when it is used as a  $\pi$ -conjugated linker between two D/A units.

We have therefore synthesized short and simple building blocks with trimer and pentamer structures. In the trimer structure, two Tz units sandwich a central unit that could be either an electron-deficient 2,1,3-benzothiadiazole (Bzt) unit or an electron-rich 3,4-ethylenedioxythiophene (EDOT) unit (Figure 1). In the pentamer structure, two end-capping groups (ECG) of opposite nature compared to the central unit (i.e., a weak methoxybenzene electron-donating group in the case of a Bzt central unit and a weak trifluoromethylbenzene electron-accepting group in the case of an EDOT central unit) were added.

For each structure, we synthesized three different regioisomers by using different Tz orientations along the conjugated backbone. We deliberately synthesized naked structures without solubilizing side chains in order to avoid any pronounced rotation of the conjugated backbone due to steric hindrance. Each synthesized compound was investigated by UV/visible absorption in solution, highlighting any difference in conjugation length due to differences in Tz orientation. Furthermore, a theoretical analysis of the different compounds

Received: August 12, 2014

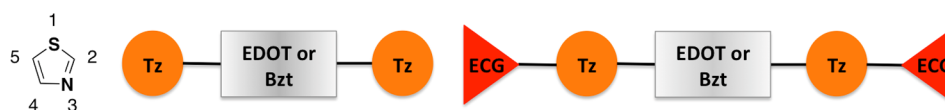


**Figure 1.** Chemical structures: Tz (thiazole), left; Tz-based trimer, center; pentamer, right. ECG: end-capping group.

using density functional theory (DFT) calculations was performed. By using such calculations, we aimed to discriminate between the influence on the absorption properties of the compounds of the position of the Tz unit (relative to the other units) and of the orientation of the Tz unit. On the basis of the experimental and theoretical data therein, we present a general guideline for the synthesis of alternating D/A-conjugated compounds using Tz.

## RESULTS AND DISCUSSION

Synthesis work starts with the synthesis of six Tz-based trimers using either electron-deficient Bzt or electron-rich EDOT as the central unit (Figure 2).

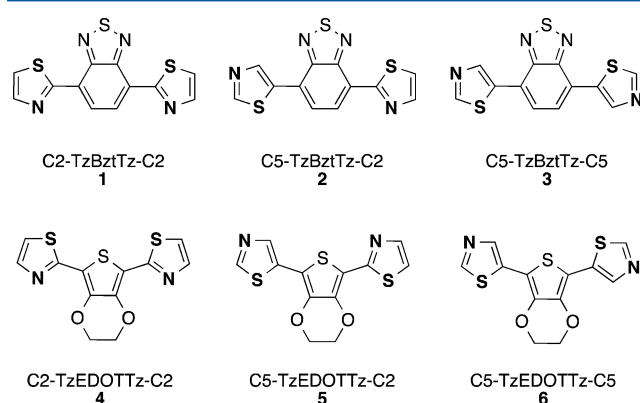


**Figure 2.** Chemical structures of regioisomer trimers based on 2,1,3-benzothiadiazole (Bzt) and 3,4-ethylenedioxythiophene (EDOT), respectively. Bzt, top; EDOT, bottom.

Most D/A-alternating conjugated materials are synthesized via Suzuki or Stille cross-coupling reactions. These methodologies first require us to obtain the organometallic and halide derivatives of the building blocks. However, in addition to a certain toxicity (especially for the trialkyltin derivatives), the synthesis of such derivatives can be overly challenging and

time-consuming for a relatively poor reaction yield because of the numerous steps required for the synthesis of organometallic reagents and to their relative instability. Recently, direct arylation has been applied to the synthesis of semiconducting molecules (small organic molecules and polymers).<sup>7–9</sup> This reaction allows for direct cross-coupling between two aromatic groups. No preliminary synthesis step is required to obtain the tin or boronic derivative of one of the synthons. Additionally, direct arylation allows for the coupling of a vast range of heterocyclic and aryl halides, which are far more numerous than boronic acid or tin derivative coupling partners.<sup>8,10</sup> However, few examples of regioselective, catalyzed CH-activation of Tz have been published so far.<sup>11–13</sup> Most often, C2-blocked Tz was used to ensure the selective C5-arylation and vice versa (Tz nomenclature in Figure 1).<sup>14</sup> Therefore, in this article, we have made an effort to develop a specific strategy for direct arylation that allows for the selective coupling of either the C2 or the C5 position, keeps the other positions unsubstituted, and results in very good to excellent yields of the isolated products.

We therefore synthesized three regioisomers based on the TzBztTz architecture by following a synthesis approach developed by Strotman et al. in 2010.<sup>15</sup> These authors published a direct-arylation methodology of oxazole that allows for highly regioselective monocoupling at either the C2 or the C5 position. This synthesis strategy is interesting because of the fact that no early protection step is required.

An initial screening with 4,7-dibromo-2,1,3-benzothiadiazole as the substrate was carried out by examining the impact of the palladium source, solvent, and ligand on the reaction yield and on C2- and C5-arylation selectivity (Table 1).

We started this study by investigating the direct arylation of Tz under optimum conditions as defined by Strotman et al.,<sup>15</sup> using Pd(OAc)<sub>2</sub> and the Cy<sub>3</sub>P ligand (L1 in Figure 3) as the catalytic system in toluene, with pivalic acid (PivOH) as an additive and Cs<sub>2</sub>CO<sub>3</sub> as the base. The choice of Cs<sub>2</sub>CO<sub>3</sub> as the base was motivated by its high solubility in organic solvents, relative to that of inorganic bases, effectively increasing the base concentration during the reaction. A substoichiometric quantity

**Table 1.** Optimization of Pd-Catalyzed C2- and C5-Selective Direct Arylation of Thiazole with 4,7-Dibromo-2,1,3-benzothiadiazole

entry	catalyst <sup>a</sup>	ligand <sup>b</sup>	solvent <sup>c</sup>	1/3 ratio <sup>d</sup>	isolated yield <sup>e</sup> 1/3
1	Pd(OAc) <sub>2</sub>	L1	toluene	85:15	50:<1
2	Pd(OAc) <sub>2</sub>	L2	toluene	90:10	58:traces
3	Pd-Herrmann	L1	toluene	90:10	65:traces
4 method A) <sup>f</sup>	Pd-Herrmann	L2	toluene	99:1	79:traces
5	Pd-Herrmann	L3	toluene	15:1	60:30
6	Pd-Herrmann	L4	toluene	1:1	
7	Pd-Herrmann	L3	DMAc	1:15	5:52
8	Pd-Herrmann	L3	DMF	1:40	<1:50
9	Pd-Herrmann	L4	DMF	1:80	traces:69
10 method B) <sup>f</sup>	Pd-Herrmann	L4	DMAc	1:99	traces:75

<sup>a</sup>5 mol % catalyst. <sup>b</sup>10 mol % ligand. <sup>c</sup>[0.1 M] dried solvent. <sup>d</sup>Ratio in the crude reaction mixture was calculated using the <sup>1</sup>H NMR results. <sup>e</sup>Isolated yield of major single-trimer regioisomer after purification in a silica-gel column and subsequent recrystallization. <sup>f</sup>Methods A and B are described in the Experimental Section.

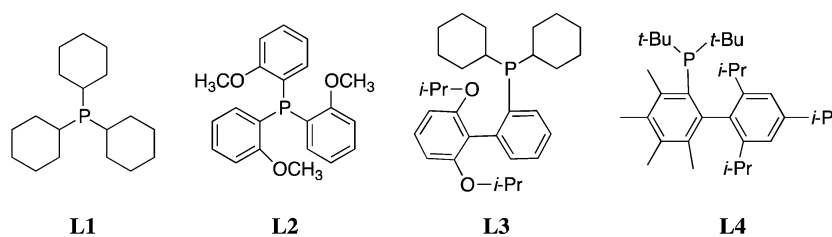
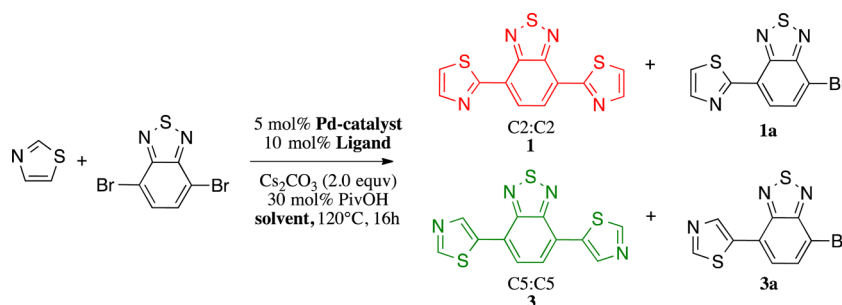


Figure 3. Ligands employed to screen the direct-arylation catalysis reaction of thiazole (Tz).

**Scheme 1. Syntheses of Isomers C2-C2(1)- and C5-C5(3)-3,4-Ethylenedioxythiophene(Bzt)-Based Trimers**



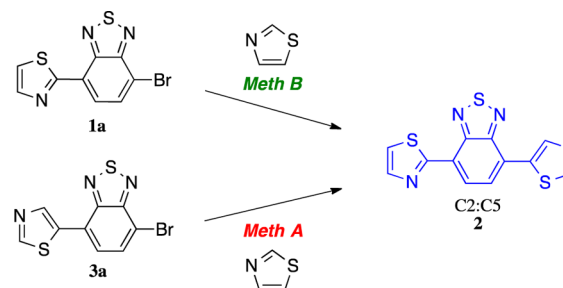
of PivOH has shown a positive impact on CH activation (i.e., acceleration of reaction rate and yield improvement).<sup>10</sup> Such conditions gave good C2 selectivity but only a moderate yield, with 50% isolated trimer and ~30% isolated monocoupling product (Table 1, entry 1).

Palladacycle complexes  $[\text{Pd}(\mu\text{-L})_2(\text{PC})_2]$  have been described in the literature as being highly efficient catalysts (e.g., in the Heck vinylation of aryl halides<sup>16</sup> or in the polycondensation using the direct-heteroarylation reaction).<sup>17</sup> Therefore, in the following reaction, we used the Pd-Herrmann complex (*trans*-di( $\mu$ -acetato)-bis[*o*-(di-*o*-tolylphosphino)-benzyl]dipalladium(II)) as the palladacycle complex in order to increase the overall reaction yield. Thus, we improved the isolated yield of C2-C2 trimer **1** to 65% by keeping the selectivity as high as possible (Table 1, entry 3). The optimal reaction conditions were obtained with tris(4-methoxyphenyl)phosphine (Figure 3, **L2**), using the method we will hereafter call method A (Table 1, entry 4); selectivity of 99:1 could be obtained for the direct arylation of C2, as well as a high yield. A subsequent change in method A to using ligand RuPhos (Figure 3, **L3**) did not lead to an optimization of the yield under the arylation reaction conditions and resulted in a large drop in selectivity (Table 1, entry 5). However, this lower selectivity allowed us to isolate properly the C5-C5 trimer regioisomer for the first time, indicating that this direct arylation is also a promising pathway for C5-C5 trimer regioisomer synthesis. Thus, keeping this ligand, we observed that a modification of the solvent to one that is more polar solvent (e.g., DMAc or DMF) leads to a direct switch of the selectivity (Table 1, entries 7 and 8) with the C5-C5 trimer regioisomer as the major product (52 and 50% of isolated C5-C5 trimer **3**, respectively). The effect of solvent polarity on regioselectivity catalysis has been already reported in recent papers.<sup>12,15</sup> Finally, changing to a more bulky ligand (i.e., tetramethyl-*t*-BuXPhos, **L4**, Figure 3) leads to an increase in selectivity for a C5-C5 trimer and in the yield of the isolated C5-C5 trimer **3** product in polar solvents (i.e., DMF or DMAc). The optimal reaction conditions were obtained with **L4**, using the method we will hereafter call method B (Table 1, entry 10); selectivities of 99:1 could be obtained for the direct

arylation of C5, as well as a high yield. In summary, the use of a more polar solvent together with a bulkier ligand considerably increases C5 selectivity, whereas high C2 selectivity has been obtained in a less-polar toluene solvent with smaller ligands. Interestingly, we did not observe any polycondensation byproducts, indicating good control over the CH-activation reaction.

The synthesis of C2-C5 trimer hybrid **2** is proof of the high regioselectivity of the direct-arylation reaction. Indeed, to obtain this trimer, we collected the monocoupling derivatives originating from the previous reactions. These bromo-dimer monoadducts (Scheme 1, products **1a** and **3a**) were then put into a reaction with Tz following methods B and A, respectively, to complete the synthesis and reach the final hybrid, compound **2**, with high yield and selectivity. The

**Scheme 2. Synthesis of the Hybrid C2-C5-2,1,3-Benzothiadiazole(Bzt)-Based Trimer 2**



regioselectivity of the direct-arylation reaction and the subsequent formation of the desired trimer were both unambiguously confirmed by single-crystal X-ray diffraction. For the description of X-ray diffraction results, the usual notation will be used (Figure 4). Trimers **1–3** were crystallized in the  $P2_1/c$  space group by the slow diffusion of methanol into saturated  $\text{CH}_2\text{Cl}_2$  or  $\text{CHCl}_3$  solutions. None of the atoms are placed on special positions in the different unit cells. Their structures reveal that the connectivity between the different aromatic rings constituting the three Tz-Bzt-Tz moieties was as

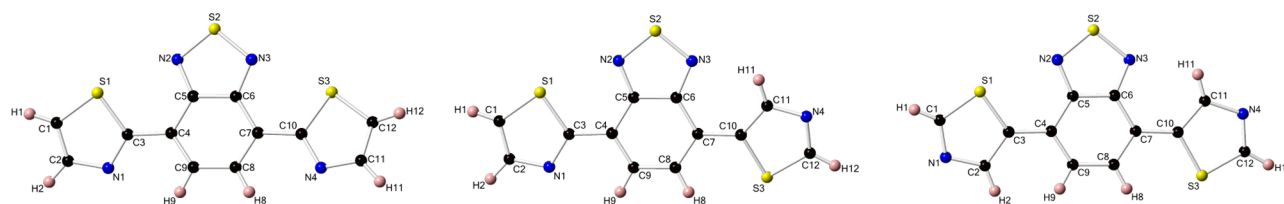
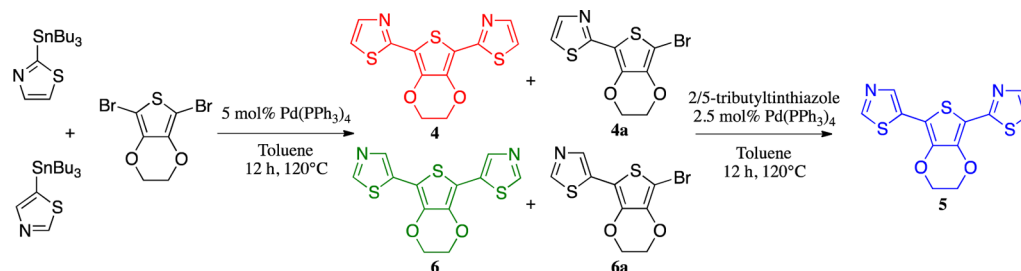
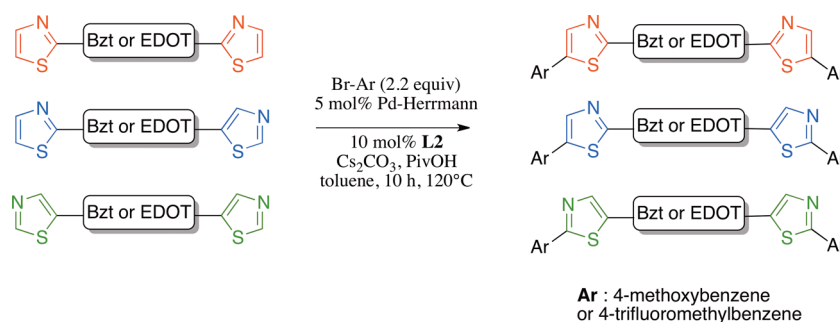


**Figure 4.** Ball-and-stick representation of trimers. Thiazole, Tz; 2,1,3-benzothiadiazole, Bzt. C2-Tz-Bzt-Tz-C2, left; <sup>18</sup> C2-Tz-Bzt-Tz-C5, middle; C5-Tz-Bzt-Tz-C5, right. Numbering of the carbon atoms in the structures depicted (including C2 and C5) is independent of the nomenclature used to differentiate trimers 1–3 as C2 or C5.

### Scheme 3. Synthesis of 3,4-Ethylenedioxythiophene(EDOT)-Based Trimers



### Scheme 4. Synthesis of 2,1,3-Benzothiadiazole(Bzt)- and 3,4-Ethylenedioxythiophene(EDOT)-Based Pentamers



expected and that they are planar (less than  $0.6^\circ$  deformation). However, the C–C aromatic bond lengths are nonequivalent in the benzyl rings of the different Tz moieties. C4–C9 and C7–C8 bond lengths range from 1.368(4) to 1.383(3) Å, whereas C4–C5, C5–C6, C6–C7, and C8–C9 bond lengths are longer, ranging from 1.410(4) to 1.444(5) Å (Figure 4). Three different unit cells (each containing four trimers) formed well-organized crystal lattices without any voids or significant sign of positional disorder associated with thermal motions of the different Bzt or Tz groups. The different lattices are stabilized by intermolecular heteroatom interactions (e.g., S...S, N...S) and/or multiple H-bonding (e.g., H...S, H...N).<sup>19,20</sup> In addition, extensive  $\pi$ -stacking interactions, following the two directions favored by the lattice symmetry, are noticeable. In the solid state, these diverse interactions, without any doubt, influence the optoelectronic properties of trimers 1–3. (Detailed descriptions can be found in the Supporting Information.)

Unfortunately, the direct-arylation reaction did not proceed when using the electron-rich 2,5-dibromo-3,4-ethylenedioxythiophene unit and naked Tz in front or when using a 3,4-ethylenedioxythiophene unit and monobrominated Tz in front. Thus, we performed a standard Stille reaction using dibromo-EDOT as well as 2-tributylthiazole and 5-tributylthiazole derivatives for the synthesis of compounds 4 and 6, respectively (Scheme 3). Both compounds were obtained in high reaction

yields. Similar to hybrid C2-C5-Bzt trimer 2, hybrid C2-C5-EDOT trimer 5 was obtained by the reaction of collected monoadduct byproducts 4a and 6a with a suitable Tz-tin derivative (Scheme 3). With the Stille coupling reaction being known to be regioselective,<sup>21</sup> no characterization by XRD was undertaken with trimers 4–6.

A first observation of the physical-chemical differences between regioisomers TzBztTz and TzEDOTTz trimers has been observed on their respective <sup>1</sup>H NMR spectra (Supporting Information, Figure S1). Indeed, an important shielding/deshielding effect between the chemical shifts of the aromatic protons could be seen depending on the isomer. More specifically, we clearly observed a pronounced deshielding effect of the remaining aromatic protons when comparing spectra of C5-C5 isomers 3 and 6 to those of C2-C2 isomers 1 and 4 (both Bzt- and EDOT-derivatives). This deshielding effect is most likely due to the more electronegative nature of C2 of Tz relative to that of C5 of Tz. Interestingly, the chemical shift of the proton in the C4 position depends on the nature of adjacent carbons with respect to each isomer structure.

To investigate further the effect of Tz-orientation on the material properties, we extended the conjugation pathway of each trimer with an end-capping group (ECG) possessing an electronic nature opposite that of the central chemical unit. Thus, in the case of the Bzt derivatives, we used a methoxybenzene group as a weak electron-donor group (D-



ECG), whereas we used a trifluoromethylbenzene group as a weak electron-acceptor group (A-ECG) in the case of the EDOT derivatives. In the pentamer structure, the Tz unit could be seen as a  $\pi$ -conjugated bridge between two moieties of opposite electronic nature.

We decided to employ the general Pd-catalyzed direct-arylation reaction to synthesize these new pentamers. Interestingly, because one  $\alpha$ -reacting position of the sulfur atom is already blocked, there is no longer a selectivity issue (considering that the C4 position is effectively less reactive), and we observed that a standard CH activation allows all coupling reactions to proceed, whatever the initial trimer or the electronic nature of the chosen ECG. We followed method A, previously used in the selective coupling of the C2 position on a Bzt central unit (Table 1, entry 4). This reaction proceeded with good yields, in the range of 60–80% in all cases (Scheme 4). This result underlines that the conditions allowing a highly regioselective coupling of C2 positions (method A) in the previous case of trimer formations do not prevent CH activation of the C5 position. In fact, under the conditions of method A, the reactivity of C2 is higher than that of C5. As soon as the C2 position is blocked and the C5 position is available, the latter is able to react under the conditions of method A. This behavior is in agreement with previous articles published by several groups under similar conditions.<sup>12,22</sup> In a manner similar to that of the trimers, large changes in chemical shifts have been observed in the <sup>1</sup>H NMR spectra with respect to the studied regioisomers (Supporting Information).

We were thus able to synthesize a series of new small molecules with Tz units, including three regioisomers that differ by the Tz orientation.

#### Absorption Properties and Theoretical Calculations.

To justify the choice of the different units, density functional theory (DFT) calculations were performed using SPARTAN<sup>23</sup> at the B3LYP/6-311+G\* level of theory in dichloromethane. For each unit, the calculated HOMO and LUMO levels are given in Table 2. From the calculation point of view, Tz,

**Table 2. Calculated HOMO and LUMO Levels for the Different Aromatic Moieties**

aromatic moiety	HOMO (eV)	LUMO (eV)
Bzt	−6.7	−2.5
EDOT	−5.8	−0.1
Tz	−6.8	−0.7
D-ECG	−5.9	−0.0
A-ECG	−7.0	−0.6

because of its lower HOMO and LUMO levels, is a clear electron acceptor compared to EDOT. Conversely, because their HOMO energy levels are quite comparable, Tz is not a pure electron-donor unit compared to Bzt, even though the LUMO level of Bzt is much lower than that of Tz. This point has already been discussed in detail elsewhere,<sup>6</sup> but calculations in the present study led to slightly different results because no solvent was taken into account in ref 6.

In the case of the methoxybenzene group as a weak electron-donor end-capping group (D-ECG), the HOMO and LUMO levels are lower compared to those of Bzt; whereas for the case of the trifluoromethylbenzene group as a weak electron-acceptor end-capping group (A-ECG), the HOMO and LUMO levels are lower compared to those of EDOT.

We performed UV/visible light absorption measurements in solution to further investigate the material properties of each regioisomer. Normalized spectra of the trimers recorded in solution in dichloromethane are displayed in Figure 5, and the corresponding optical data is shown in Table 3. As expected, for each system, the three regioisomers show similar absorption spectra, especially when they are normalized as in Figure 5. However, significant variations in the position and small variations in the amplitude of the absorption peaks are observed. Indeed, regarding the Bzt derivatives (Figure 5a), the C2-C2 regioisomer exhibits a clear bathochromic shift of its maximum absorption wavelength, as compared to that of the C5-C5 regioisomer. This redshift indicates a favored  $\pi$ -conjugation pathway when the Tz is coupled to the benzothiadiazole in the C2 position. This result is in agreement with the fact that the hybrid C2-C5 regioisomer shows an intermediate position of its maximum absorption wavelength. The results for EDOT-based trimers are exactly the same, with the C2-C2 regioisomer being the most conjugated and the C5-C5 regioisomer less conjugated. This experimental observation contradicts what we anticipated intuitively. Indeed, the Tz ring has one electron-rich carbon atom (C5) and one electron-poor carbon atom (C2) (Figure 1).<sup>1</sup> We thought that when the C5 carbon of Tz was linked to the electron-rich moiety (or, conversely, when the C2 carbon of Tz was linked to the electron-deficient moiety), the trimer would be more conjugated (hereafter referred to as the matching case). By this same logic, we thought that when the C2 carbon of Tz was linked to the electron-rich moiety (or, conversely, the C5 carbon of Tz was linked to the electron-deficient moiety), the trimer would be less conjugated (hereafter referred to as the mismatching case).

In other words, for the Bzt-based trimers, because we considered Tz to be electron-rich when compared to Bzt, we thought that the C2-C2 regioisomer (matching case) would be more conjugated than the C2-C5 regioisomer and that the C2-C5 regioisomer would be more conjugated than the C5-C5 regioisomer (mismatching case). Likewise, we anticipated the opposite trend for EDOT-based trimers because we considered Tz to be electron-deficient when compared to EDOT, whereas experimentally, the C2-C2 regioisomer (i.e., mismatching case) is also the most conjugated for EDOT-based trimers.

To understand this nonintuitive experimental behavior, we performed HOMO and LUMO DFT calculations in dichloromethane. UV/visible spectra were also calculated using SPARTAN, and the absorption maxima, as well as the calculated energy gap, are given in Table 4. Comparing the calculated results (Table 4) and the experimental ones (Table 3), it appears that, despite the usually observed shift between the calculated and experimental optical band gap, the calculated results are fully consistent with the experimental ones. For the Bzt-based trimers as for the EDOT-based trimers, the C2-C2 regioisomer is always more conjugated than the C2-C5 one, with the C2-C5 regioisomer being more conjugated than the C5-C5 regioisomer. The calculated HOMO and LUMO frontier orbitals in the minimized-energy configuration for C2-C2 and C5-C5 regioisomers are shown in Figures 6 and 7 for Bzt-based and EDOT-based trimers, respectively.

The electron-rich (C5) and electron-poor (C2) carbons of the Tz ring substantially influence the frontier orbitals of the Bzt-based trimers. Indeed, when C2 is at the extremity of the trimers (C5-TzBztTz-C5 case), the HOMO appears to be less electron-dense on both sides of the trimers (Figure 6, circled

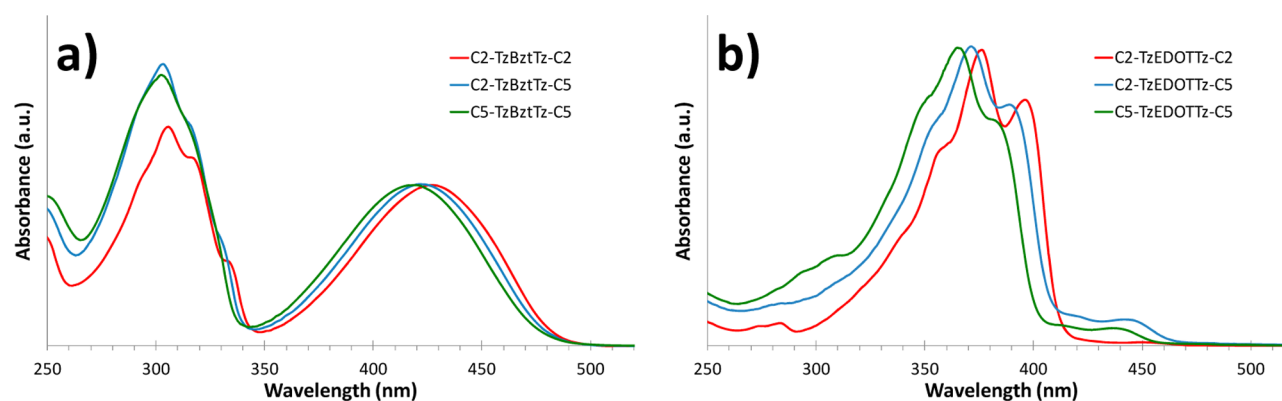


Figure 5. UV/visible absorption spectra in dichloromethane solution: Bzt-based trimers, a; EDOT-based trimers, b.

Table 3. Optical Properties of Thiazole-Based Trimers

compound	$\lambda_{\max}$ (nm)	$\lambda_{\text{offset}}$ (nm)	optical band gap (eV)	offset absorption shift (nm)
C2-TzBztTz-C2	428.5	474.4	2.61	
C2-TzBztTz-C5	423.5	470.0	2.64	−4.4
C5-TzBztTz-C5	419.5	465.0	2.67	−5.0
C2-TzEDOTTz-C2	377.5	411.8	3.01	
C2-TzEDOTTz-C5	373.0	408.2	3.04	−3.6
C5-TzEDOTTz-C5	367.5	403.0	3.07	−5.2

Table 4. Calculated Optical Properties of Thiazole-Based Trimers

compound	$\lambda_{\max}$ (nm)	optical band gap (eV)	offset absorption shift (nm)
C2-TzBztTz-C2	459.9	2.87	
C2-TzBztTz-C5	456.8	2.89	−3.1
C5-TzBztTz-C5	452.6	2.93	−4.3
C2-TzEDOTTz-C2	357.6	3.39	
C2-TzEDOTTz-C5	355.0	3.42	−2.5
C5-TzEDOTTz-C5	353.3	3.44	−1.7

area in the HOMO), and the same holds for the LUMO in the central part (Figure 6, circled area in the LUMO). In addition, the DFT calculations indicate a clear involvement of the sulfur atom in the conjugation pathway in the case of the C2-TzBztTz-C2 trimer, which is not the case for the C5-TzBztTz-C5 isomer. Therefore, the C5-TzBztTz-C5 trimer appears to be

less conjugated because of less delocalization of the frontier orbitals. The same conclusions can be drawn for the EDOT-based trimer's HOMO (Figure 7, circled part of the HOMO), whereas no impact on the EDOT-based trimer's LUMO appears in Figure 7. From the calculated frontier energy levels, it can also be understood that the C5-TzEDOTTz-C5 regioisomer is less conjugated than the C2-TzEDOTTz-C2 regioisomer.

From the experimental and calculation results on the trimers, it appears that the C2-C2 regioisomers are always more conjugated than the C5-C5 ones, even though the central unit is changed from being electron-accepting (Bzt) to electron-donating (EDOT) relative to the Tz moieties. The most probable hypothesis based on the calculations is the better  $\pi$  orbitals overlap in the case of the C2-C2 isomer with, in particular, a delocalization over all of the Tz-constituent atoms, including the sulfur atom. The intermediate case of C2-C5 regioisomers is thus easily understood with a C2-bonded Tz on one side and a C5-bonded Tz on the other.

Regarding the pentamer series, Tz bridges an electron-rich and an electron-deficient moiety. We developed a new “color nomenclature” to facilitate reading. If the electron-rich carbon in the Tz ring (C5) is linked to the electron-rich moiety and consequently the electron-poor carbon in the Tz ring (C2) is linked to the electron-deficient moiety, then the bond is illustrated using green. In the opposite case, the bond is illustrated using red. We highlight that a green bond

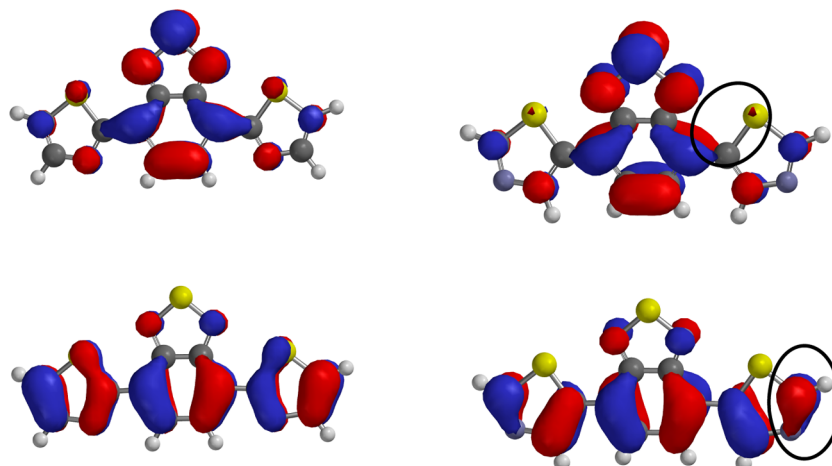


Figure 6. Calculated LUMO (top) and HOMO (bottom) orbitals for C2-TzBztTz-C2 (left) and C5-TzBztTz-C5 (right).

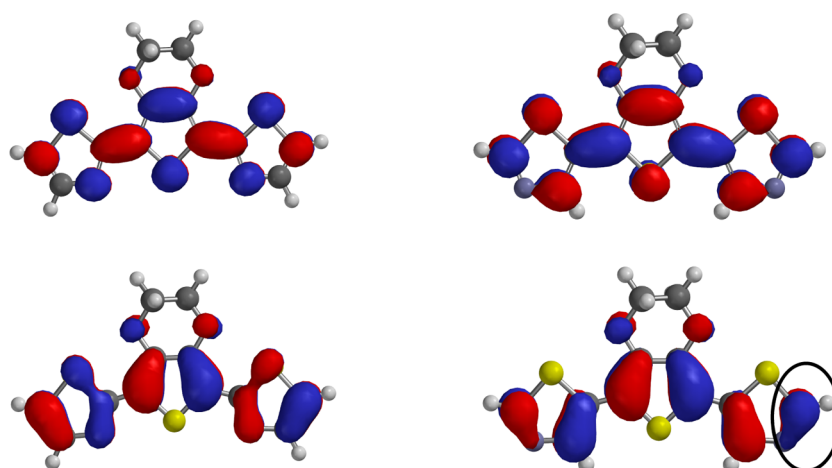


Figure 7. Calculated LUMO (top) and HOMO (bottom) orbitals for C2-TzEDOTTz-C2 (left) and C5-TzEDOTTz-C5 (right).

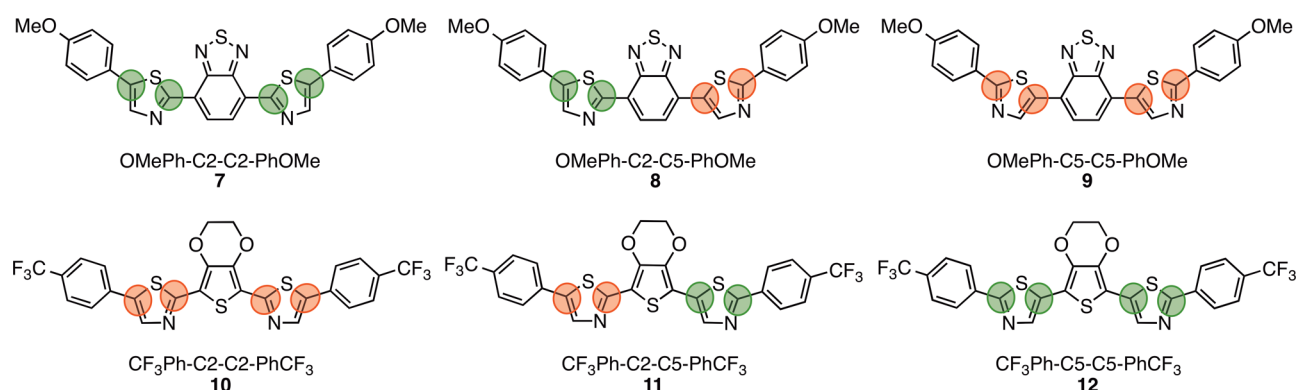


Figure 8. Chemical structures of the studied pentamers with color nomenclature. Matching bonds, green; mismatching bonds, red.

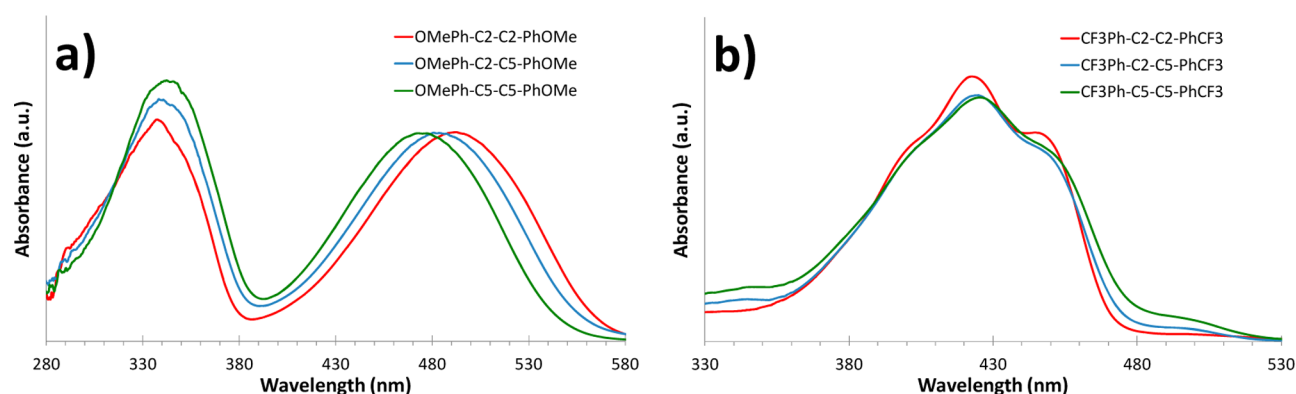


Figure 9. UV/visible absorption spectra in dichloromethane solution. 2,1,3-Benzothiadiazole-based pentamers, a; 3,4-ethylenedioxythiophene-based pentamers, b.

corresponds to the matching case (where the Tz dipole reinforces the dipole of the linked moieties) whereas a red bond corresponds to the mismatching case (where the Tz dipole weakens the dipole of the linked moieties).<sup>1</sup> This color nomenclature is used in Figure 8 for compounds 7–12. The color nomenclature more clearly shows that pentamer 7 should be the most conjugated in the Bzt-based series, whereas pentamer 12 should be the most conjugated in the EDOT-based series.

UV/visible absorption spectra in dilute dichloromethane solution are presented in Figure 9. It clearly appears from the UV/visible spectra that the trend observed for trimers is not

valid for pentamers. As intuitively anticipated for the Bzt-based pentamers, the C2-C2 regioisomer is the most conjugated material, the C5-C5 regioisomer is the less conjugated material, and the C2-C5 regioisomer lies in between. Likewise, for the EDOT-based pentamer, the C2-C2 isomer becomes the less-conjugated species, whereas the C5-C5 isomer is the most conjugated and the C2-C5 regioisomer lies in between (Table 5). There are two main differences between the trimer and the pentamer cases. For the trimers, Tz is at the extremity of the molecule and is used as an electron-deficient unit or electron-rich unit relative to EDOT or Bzt, respectively. For the pentamers, Tz is no longer at the extremity of the molecule and

Table 5. Optical Properties of Thiazole-Based Pentamers

compound	$\lambda_{\max}$ (nm)	$\lambda_{\text{offset}}$ (nm)	optical band gap (eV)	offset absorption shift (nm)
OMePh-C2-C2-PhOMe (7)	492	566.4	2.19	
OMePh-C2-C5-PhOMe (8)	487	555.4	2.23	−11
OMePh-C5-C5-PhOMe (9)	479	545.4	2.27	−10
CF <sub>3</sub> Ph-C2-C2-CF <sub>3</sub> Ph (10)	424	460	2.69	
CF <sub>3</sub> Ph-C2-C5-CF <sub>3</sub> Ph (11)	426	465	2.67	+5
CF <sub>3</sub> Ph-C5-C5-CF <sub>3</sub> Ph (12)	427	470	2.64	+5

is used as a linker between electron-rich and/or electron-deficient moieties. The experimental observation made for trimers (C2-C2 as the most conjugated isomer for both Bzt- and EDOT-based materials) is probably mainly due to the fact that the trimers are short molecules with a strong effect of the orientation of Tz on the frontier orbitals' delocalization. For longer molecules, when Tz is used as a linker between electron-rich and/or electron-poor moieties the conjugation length of the final molecule is directly linked to the orientation of the Tz group.

In other words, a careful choice (based on the synthesis paths presented in this study) of the orientation of Tz allows an increase in the conjugation length of the synthesized molecule if a simple rule is taken into account: the electron-rich carbon of Tz (C5) must be oriented toward the electron-donor moiety, whereas the electron-poor carbon of Tz (C2) must be oriented toward the electron-acceptor moiety. This general rule is not valid for trimers where the Tz unit sandwiches an electron-rich or an electron-deficient unit. In this specific case, the C2-C2 regioisomer is always the most conjugated material.

## CONCLUSIONS

We have demonstrated that selective CH activation can be successfully applied to the synthesis of Tz-based materials, avoiding any protection step. We have applied this strategy to the synthesis of a series of trimers in which the Tz group sandwiches either an electron-rich unit (EDOT) or an electron-deficient (Bzt) unit and the Tz group has a regioselective orientation. We have applied the same strategy to the synthesis of a series of pentamers where the Tz group is used as a  $\pi$ -conjugated bridge between an electron-rich central unit and electron-deficient end-capping groups and vice versa. On both trimers and pentamers, we have investigated the effect of Tz orientation on the absorption properties of the materials. Tz has one electron-rich carbon (C5) and one electron-deficient carbon (C2). When C5 and C2 are covalently bonded to an electron-rich unit and an electron-deficient unit, respectively, the Tz orientation follows the matching case. In the opposite configuration, the Tz orientation follows the mismatching case.

For pentamers, the matching case leads to the most conjugated materials, whereas the mismatching case leads to those that are less conjugated.

For trimer molecules where Tz is an ECG (i.e., having only one covalent bond), the C2-grafted position always leads to the most conjugated material, even if the central unit is electron-rich compared to Tz. Density functional theory calculations support this nonintuitive behavior because the C5 trimers frontier orbitals are less delocalized than their C2 counterparts.

The present work gives chemical synthesis tools for the synthesis of selectively oriented Tz-based materials as well as a

general guideline for the design of Tz-based materials with the longest conjugation length.

## EXPERIMENTAL SECTION

All reagents and chemicals were purchased from commercial sources. THF, Et<sub>2</sub>O, and toluene were distilled from Na/benzophenone. Thiazole (Tz), 2,5-dibromo-3,4-ethylenedioxythiophene, tricyclohexylphosphine (L1), tris(*o*-methoxyphenyl)phosphine (L2), 2-dicyclohexylphosphino-2',6'-diisopropoxybiphenyl (RuPhos-L3), 3,4,5,6-tetramethyl-*t*-Bu-X-Phos (L4), and other reagents and chemicals were used as received. 4,7-Dibromobenzo[c][1,2,5]thiadiazole, *trans*-di( $\mu$ -acetato)bis[*o*-(di-*o*-tolyl-phosphino)benzyl]dipalladium(II), Pd(PPh<sub>3</sub>)<sub>4</sub>, and 2-tributylstannyl Tz were prepared as described in the literature.<sup>24,25</sup>

<sup>1</sup>H and <sup>13</sup>C NMR spectra were recorded on 300 and 400 MHz NMR spectrometers, respectively; <sup>1</sup>H and <sup>13</sup>C chemical shifts were reported in parts per million ( $\delta$ ) relative to CDCl<sub>3</sub> (7.26 and 77.2, respectively) or 1,1,2,2-tetrachloroethane-*d*<sub>2</sub> (6.02 and 73.8, respectively). Melting points were determined in open capillary tubes on a melting-point apparatus. UV/visible absorption spectroscopy measurements were performed using a scanning spectrophotometer. For the X-ray diffraction studies, the intensity data were collected at 173(2) K on an APEX2 CCD diffractometer (monochromated Mo *K* $\alpha$  radiation,  $\lambda$  = 0.71073 Å). The structures were solved by direct methods (SHELXS-97) and refined by full-matrix least-squares procedures (based on F<sup>2</sup>, SHELXL-97) with anisotropic thermal parameters of all the non-hydrogen atoms. The hydrogen atoms were introduced into the geometrically calculated positions (SHELXL-97 procedures) and refined by riding on the corresponding parent atoms.

**Synthesis of Trimers by Pd-Catalyzed CH-Selective Direct Arylation. Method A (C2 Position).** A flame-dried Schlenk flask was charged with a brominated derivative (1.0 equiv), Pd-Herrmann (0.05 equiv), and ligand solution: tris(*o*-methoxyphenyl)phosphine L2 (0.1 equiv), Cs<sub>2</sub>CO<sub>3</sub> (2.2 equiv), and PivOH (0.3 equiv). Dried and degassed toluene (0.2 M) was added under inert gas, followed by Tz (2.0 equiv), and the mixture was stirred for 16 h at 120 °C. After cooling to room temperature, the reaction mixtures were evaporated under reduced pressure and purified first by column chromatography (silica gel, CH<sub>2</sub>Cl<sub>2</sub>/EtOAc = 90:10) and finally by recrystallization in CHCl<sub>3</sub>/MeOH.

**4,7-Di(thiazol-2-yl)benzo[c][1,2,5]thiadiazole (1).** Molecular weight 302.4 g/mol; orange solid; mp = 244–245 °C; method A yield 79%; <sup>1</sup>H NMR (300 MHz, CDCl<sub>3</sub>)  $\delta$  = 8.74 (s, 1H), 8.06 (d, *J* = 3.2 Hz, 1H), 7.63 (d, *J* = 3.2 Hz, 1H); <sup>13</sup>C NMR (75 MHz, CDCl<sub>3</sub>)  $\delta$  = 161.9, 152.0, 143.5, 127.4, 126.6, 122.3; IR (cm<sup>−1</sup>) 3113, 3068, 1543, 1465, 1311, 1270, 1220, 1164, 1143, 1070, 1050, 871, 863, 850, 763, 734, 716, 689, 659, 600; HRMS ESI-TOF *m/z* calculated for C<sub>12</sub>H<sub>7</sub>N<sub>4</sub>S<sub>3</sub> [M − H], 302.9827; found, 302.9839.

**4-Bromo-7-(thiazol-2-yl)benzo[c][1,2,5]thiadiazole (1a).** Molecular weight 298.2 g/mol; yellow solid; mp = 169–170 °C; method A yield 34%; <sup>1</sup>H NMR (300 MHz, CDCl<sub>3</sub>)  $\delta$  = 8.48 (d, *J* = 7.8 Hz, 1H), 8.02 (d, *J* = 3.2 Hz, 1H), 7.97 (d, *J* = 7.8 Hz, 1H), 7.60 (d, *J* = 3.2 Hz, 1H); <sup>13</sup>C NMR (75 MHz, CDCl<sub>3</sub>)  $\delta$  = 161.6, 153.6, 151.3, 143.3, 132.4, 127.6, 125.6, 122.2, 115.5; IR (cm<sup>−1</sup>) 3102, 3071, 1526, 1486, 1471, 1317, 1306, 1274, 1116, 1050, 935, 877, 871, 856, 845, 762, 736, 648, 548. MS ESI-TOF *m/z* (%) calculated for [M − Na] C<sub>9</sub>H<sub>4</sub>BrN<sub>3</sub>S<sub>2</sub>Na, 319.89; found, 319.89 (80), 321.89 (100).

**4-(Thiazol-2-yl)-7-(thiazol-5-yl)benzo[c][1,2,5]thiadiazole (2).** Molecular weight 302.4 g/mol; orange solid; mp = 203–205 °C; method A or method B yield around 72% on average; <sup>1</sup>H NMR (300 MHz, CDCl<sub>3</sub>)  $\delta$  = 8.94 (s, 1H), 8.88 (s, 1H), 8.62 (d, *J* = 7.7 Hz, 1H), 8.02 (d, *J* = 3.2 Hz, 1H), 7.96 (d, *J* = 7.7 Hz, 1H), 7.60 (d, *J* = 3.2 Hz, 1H); <sup>13</sup>C NMR (75 MHz, CDCl<sub>3</sub>)  $\delta$  = 161.9, 154.2, 152.2, 152.0, 143.3, 143.2, 134.1, 127.3, 126.8, 125.4, 125.4, 122.1; IR (cm<sup>−1</sup>) 3075, 3064, 1543, 1519, 1467, 1401, 1357, 1300, 1290, 1266, 1245, 1157, 1130, 1067, 873, 845, 788, 767, 720, 689, 650, 618, 595, 577; HRMS ESI-TOF *m/z* calculated for C<sub>12</sub>H<sub>7</sub>N<sub>4</sub>S<sub>3</sub> [M − H], 302.9827; found, 302.9847.



**Method B (C5 Position).** A flame-dried Schlenk flask was charged with brominated derivative (1.0 equiv), Pd-Herrmann (0.05 equiv), and ligand solution: 3,4,5,6-tetramethyl-*t*-Bu-X-Phos L4 (0.10 equiv),  $\text{Cs}_2\text{CO}_3$  (2.2 equiv), and PivOH (0.3 equiv). Dry and degassed DMAc (0.2 M) was added under inert gas, followed by Tz (2.0 equiv), and the mixture was stirred for 16 h at 120 °C. After cooling to room temperature, the reaction mixtures were extracted with  $\text{CH}_2\text{Cl}_2$  and water (3×). The organic phase was dried over  $\text{Na}_2\text{SO}_4$ , filtered, evaporated under reduced pressure, and purified by column chromatography (silica gel,  $\text{CH}_2\text{Cl}_2/\text{EtOAc}$  = 90:10) and recrystallization in  $\text{CHCl}_3/\text{MeOH}$ .

**4,7-Di(thiazol-5-yl)benzo[*c*][1,2,5]thiadiazole (3).** Molecular weight 302.4 g/mol; orange solid; mp = 186–188 °C; method B yield 75%;  $^1\text{H}$  NMR (300 MHz,  $\text{CDCl}_3$ )  $\delta$  = 8.92 (s, 1H), 8.82 (s, 1H), 7.87 (s, 1H);  $^{13}\text{C}$  NMR (75 MHz,  $\text{CDCl}_3$ )  $\delta$  = 154.0, 152.3, 142.9, 134.0, 126.8, 124.2; IR ( $\text{cm}^{-1}$ ) 3075, 1544, 1496, 1461, 1389, 1357, 1300, 1272, 1243, 1162, 1132, 1116, 1075, 1014, 873, 835, 817, 793, 746, 729, 677, 618, 599, 588; HRMS ESI-TOF  $m/z$  calculated for  $\text{C}_{12}\text{H}_7\text{N}_4\text{S}_3$  [ $\text{M} - \text{H}$ ], 302.9827; found, 302.9842.

**4-Bromo-7-(thiazol-5-yl)benzo[*c*][1,2,5]thiadiazole (3a).** Molecular weight 298.2 g/mol; yellow solid; mp = 157–158 °C; method B yield 28%;  $^1\text{H}$  NMR (300 MHz,  $\text{CDCl}_3$ )  $\delta$  = 8.92 (s, 1H), 8.78 (s, 1H), 7.86 (d,  $J$  = 7.7 Hz, 1H), 7.71 (d,  $J$  = 7.7 Hz, 1H);  $^{13}\text{C}$  NMR (75 MHz,  $\text{CDCl}_3$ )  $\delta$  = 154.0, 153.6, 151.6, 143.0, 133.6, 132.1, 127.0, 124.2, 113.8; IR ( $\text{cm}^{-1}$ ) 3118, 3080, 1583, 1526, 1500, 1479, 1384, 1272, 1114, 937, 879, 867, 841, 828, 790, 728, 626, 593, 547. MS ESI-TOF  $m/z$  (%) calculated for [ $\text{M} - \text{Na}$ ]  $\text{C}_9\text{H}_4\text{BrN}_3\text{S}_2\text{Na}$ , 319.89; found, 319.87 (80), 321.89 (100).

**5-Tributylstannylthiazole.** For the preparation of a lithium diisopropylamine (LDA) solution, *n*-butyllithium (2.5 M in hexanes, 17.6 mL, 44 mmol) was dropwise added to a solution of redistilled diisopropylamine (6.7 mL, 48 mmol) dissolved in 100 mL of dry THF at 0 °C under an argon atmosphere. The reaction was stirred at 0 °C for 15 min before being cooled to –78 °C. Then tributyltin chloride (6 mL, 22 mmol) dissolved in 20 mL of dry THF was slowly added to the LDA solution, and the reaction was stirred for 15 min. Finally, Tz (1.7 g, 20 mmol) dissolved in 20 mL of dry THF was added dropwise at –78 °C. The resulting solution was stirred overnight at room temperature under argon. Water was then added under vigorous stirring. The mixture was extracted with ethyl acetate, and the organic phase was washed with water and dried over sodium sulfate. The solvent was removed under reduced pressure, and the crude product was purified by column chromatography (silica gel pretreated with 2% triethylamine  $\text{CH}_2\text{Cl}_2$ : 100) to give 5-tributylstannylthiazole.  $^1\text{H}$  NMR (300 MHz,  $\text{CDCl}_3$ )  $\delta$  = 9.08 (s, 1H), 7.88 (t, 1H), 1.60–1.49 (m, 6H), 1.40–1.26 (m, 6H), 1.18–1.10 (pseudo-t, 6H), 0.93–0.85 (pseudo-t, 9H);  $^{13}\text{C}$  NMR (75 MHz,  $\text{CDCl}_3$ )  $\delta$  = 157.4, 149.8, 127.4, 28.8, 27.1, 13.6, 11.0.

**Method C (Stille Cross-Coupling Method).** A flame-dried Schlenk flask was charged with 2,5-dibromo-3,4-ethylenedioxythiophene (1.0 equiv). Anhydrous and degassed toluene (0.1 M) was added under inert gas, followed by 5,2-tributylstannyl thiazole (inverse) (in the case of monobromo-EDOT, 1.1 equiv; in the case of dibromo-EDOT, 2.2 equiv). Finally,  $\text{Pd}(\text{PPh}_3)_4$  (0.05 equiv) was added in one portion, and the mixture was stirred 12 h at 120 °C. After cooling to room temperature, the reaction mixtures were evaporated under reduced pressure and purified by column chromatography (silica gel,  $\text{CH}_2\text{Cl}_2/\text{EtOAc}$  = 90:10) and recrystallization in  $\text{CH}_2\text{Cl}_2$ /petroleum ether (PE).

**5,7-Di(thiazol-2-yl)-2,3-dihydrothieno[3,4-*b*][1,4]dioxine (4).** Molecular weight 308.40 g/mol; yellow-orange solid; mp = 219–220 °C; method C yield 68%;  $^1\text{H}$  NMR (300 MHz,  $\text{CDCl}_3$ )  $\delta$  = 7.80 (d,  $J$  = 3.3 Hz, 1H), 7.31 (d,  $J$  = 3.3 Hz, 1H), 4.51 (s, 2H);  $^{13}\text{C}$  NMR (75 MHz,  $\text{CDCl}_3$ )  $\delta$  = 158.0, 142.5, 139.8, 118.5, 113.6, 65.4; IR ( $\text{cm}^{-1}$ ) 3052, 1530, 1475, 1458, 1445, 1422, 1363, 1320, 1283, 1156, 1134, 1074, 1055, 962, 870, 849, 756, 705, 697, 638, 621, 562, 545; HRMS ESI-TOF  $m/z$  calculated for  $\text{C}_{12}\text{H}_9\text{N}_2\text{O}_2\text{S}_3$  [ $\text{M} - \text{H}$ ], 308.9821; found, 308.9828.

**5-(7-(Thiazol-2-yl)-2,3-dihydrothieno[3,4-*b*][1,4]dioxin-5-yl)-thiazole (5).** Molecular weight 308.40 g/mol; yellow-orange solid; mp

= 165–166 °C; method C yield 68%;  $^1\text{H}$  NMR (300 MHz,  $\text{CDCl}_3$ )  $\delta$  = 8.73 (s, 1H), 8.12 (s, 1H), 7.76 (d,  $J$  = 3.3 Hz, 1H), 7.32 (d,  $J$  = 3.3 Hz, 1H), 4.49 (m, 2H), 4.46 (m, 2H);  $^{13}\text{C}$  NMR (75 MHz,  $\text{CDCl}_3$ )  $\delta$  = 157.9, 151.5, 142.2, 140.2, 139.5, 138.2, 129.2, 118.3, 111.2, 109.5, 65.4, 65.1; IR ( $\text{cm}^{-1}$ ) 3079, 3059, 1534, 1486, 1475, 1448, 1364, 1298, 1282, 1237, 1155, 1135, 1082, 960, 879, 868, 846, 774, 754, 737, 710, 697, 631, 606, 562, 541; HRMS ESI-TOF  $m/z$  calculated for  $\text{C}_{12}\text{H}_9\text{N}_2\text{O}_2\text{S}_3$  [ $\text{M} - \text{H}$ ], 308.9821; found, 308.9831.

**5,7-Di(thiazol-5-yl)-2,3-dihydrothieno[3,4-*b*][1,4]dioxine (6).** Molecular weight 308.40 g/mol; yellow-brown solid; mp = 150–152 °C; method C yield 72%;  $^1\text{H}$  NMR (300 MHz,  $\text{CDCl}_3$ )  $\delta$  = 8.68 (s, 1H), 8.02 (s, 1H), 4.37 (s, 2H);  $^{13}\text{C}$  NMR (75 MHz,  $\text{CDCl}_3$ )  $\delta$  = 151.1, 138.9, 138.4, 129.0, 106.7, 65.0; IR ( $\text{cm}^{-1}$ ) 3084, 3069, 1534, 1474, 1449, 1398, 1368, 1299, 1279, 1232, 1077, 1007, 974, 965, 875, 840, 828, 772, 750, 693, 632, 603, 580; HRMS ESI-TOF  $m/z$  calculated for  $\text{C}_{12}\text{H}_9\text{N}_2\text{O}_2\text{S}_3$  [ $\text{M} - \text{H}$ ], 308.9821; found, 308.9836.

**Synthesis of Pentamers by Pd-Catalyzed Direct Arylation (Method A).** Following method A, 4,7-di(thiazol-5-yl)-benzo[*c*][1,2,5]-thiadiazole or 5,7-di(thiazol)-2,3-dihydrothieno[3,4-*b*][1,4]dioxine (1.0 equiv) was mixed with aryl bromide, 1-bromo-4-methoxybenzene, or 1-bromo-4-trifluoromethylbenzene (2.4 equiv) to afford the pentamer product. The pentamers were then purified by column chromatography (silica gel,  $\text{CH}_2\text{Cl}_2$ /toluene/MeOH = 80:10:10, respectively) and recrystallization in  $\text{CHCl}_3/\text{MeOH}$ .

**4,7-Bis(5-(4-methoxyphenyl)thiazol-2-yl)benzo[*c*][1,2,5]-thiadiazole (7).** Molecular weight 514.6 g/mol; dark-red solid; mp = 280–281 °C; method A yield 74%;  $^1\text{H}$  NMR (400 MHz,  $\text{CDCl}_3$ )  $\delta$  = 8.71 (s, 1H), 8.11 (s, 1H), 7.64 (d,  $J$  = 8.6 Hz, 2H), 6.98 (d,  $J$  = 8.6 Hz, 2H);  $^{13}\text{C}$  NMR (101 MHz,  $\text{CDCl}_3$ )  $\delta$  = 160.2, 159.8, 152.0, 142.7, 138.3, 128.1(×2), 126.9, 126.6, 124.1, 114.7(×2), 55.4; IR ( $\text{cm}^{-1}$ ) 1602, 1530, 1478, 1461, 1407, 1291, 1248, 1235, 1188, 1152, 1114, 1058, 1030, 885, 848, 832, 812, 794, 767, 655, 645, 632, 585, 560; HRMS ESI-TOF  $m/z$  calculated for  $\text{C}_{26}\text{H}_{19}\text{N}_4\text{O}_2\text{S}_3$  [ $\text{M}$ ], 515.0665; found, 515.0639.

**4-(5-(4-Methoxyphenyl)thiazol-2-yl)-7-(2-(4-methoxyphenyl)thiazol-5-yl)benzo[*c*][1,2,5]thiadiazole (8).** Molecular weight 514.6 g/mol; dark-red solid; mp = 234–235 °C; method A yield 68%;  $^1\text{H}$  NMR (300 MHz,  $\text{CDCl}_3$ )  $\delta$  = 8.81 (s, 1H), 8.62 (d,  $J$  = 7.8 Hz, 1H), 8.09 (s, 1H), 8.00 (d,  $J$  = 8.8 Hz, 2H), 7.96 (d,  $J$  = 7.8 Hz, 1H), 7.64 (d,  $J$  = 8.8 Hz, 2H), 7.00 (d,  $J$  = 8.7 Hz, 2H), 6.97 (d,  $J$  = 8.7 Hz, 2H);  $^{13}\text{C}$  NMR (101 MHz,  $\text{CDCl}_3$ )  $\delta$  = 169.2, 161.5, 160.0, 159.8, 152.3, 152.0, 143.7, 142.3, 138.1, 133.2, 128.2, 128.1, 126.8, 126.5, 126.2, 125.6, 125.1, 124.1, 114.6, 114.4, 55.5, 55.4; IR ( $\text{cm}^{-1}$ ) 1607, 1576, 1527, 1476, 1430, 1413, 1304, 1280, 1251, 1180, 1172, 1154, 1105, 1065, 1035, 1024, 899, 852, 841, 819, 794, 769, 757, 644, 626, 606, 583; HRMS ESI-TOF  $m/z$  calculated for  $\text{C}_{26}\text{H}_{19}\text{N}_4\text{O}_2\text{S}_3$  [ $\text{M}$ ], 515.0665; found, 515.0638.

**4,7-Bis(2-(4-methoxyphenyl)thiazol-5-yl)benzo[*c*][1,2,5]-thiadiazole (9).** Molecular weight 514.6 g/mol; red solid; mp = 222–224 °C; method A yield 67%;  $^1\text{H}$  NMR (400 MHz,  $\text{CDCl}_3$ )  $\delta$  = 8.73 (s, 1H), 7.97 (d,  $J$  = 8.8 Hz, 2H), 7.85 (s, 1H), 6.98 (d,  $J$  = 8.8 Hz, 2H);  $^{13}\text{C}$  NMR (101 MHz,  $\text{CDCl}_3$ )  $\delta$  = 168.8, 161.6, 152.4, 143.2, 133.2, 128.2(×2), 126.6, 126.2, 124.2, 114.5(×2), 55.4; IR ( $\text{cm}^{-1}$ ) 1602, 1573, 1519, 1470, 1455, 1428, 1407, 1302, 1252, 1171, 1158, 1106, 1026, 871, 854, 833, 815, 753, 675, 631, 623, 607, 588; HRMS ESI-TOF  $m/z$  calculated for  $\text{C}_{26}\text{H}_{19}\text{N}_4\text{O}_2\text{S}_3$  [ $\text{M}$ ], 515.0665; found, 515.0693. (For trifluoromethylbenzene derivatives, insufficient solubility did not allow us to perform efficient  $^{13}\text{C}$  NMR characterizations.)

**5,7-Bis(5-(4-(trifluoromethyl)phenyl)thiazol-2-yl)-2,3-dihydrothieno[3,4-*b*][1,4]dioxine (10).** Molecular weight 596.59 g/mol; light-orange solid; mp = 300–301 °C; method A yield 62%;  $^1\text{H}$  NMR (400 MHz, 80 °C,  $\text{C}_6\text{D}_2\text{Cl}_4$ )  $\delta$  = 8.12 (s, 1H), 7.79 (d,  $J$  = 8.3 Hz, 2H), 7.75 (d,  $J$  = 8.6 Hz, 2H), 4.63 (s, 2H); IR ( $\text{cm}^{-1}$ ) 1615, 1596, 1461, 1430, 1413, 1320, 1282, 1234, 1172, 1112, 1067, 1013, 962, 879, 849, 834, 756, 696, 639, 594; HRMS ESI-TOF  $m/z$  calculated for  $\text{C}_{26}\text{H}_{15}\text{F}_6\text{N}_2\text{O}_2\text{S}_3$  [ $\text{M}$ ], 597.0194; found, 597.0181.

**2-(4-(Trifluoromethyl)phenyl)-5-(7-(5-(4-(trifluoromethyl)phenyl)thiazol-2-yl)-2,3-dihydrothieno[3,4-*b*][1,4]dioxin-5-yl)thiazole (11).** Molecular weight 596.59 g/mol; light-orange solid; mp = 295–296

°C; method A yield 62%;  $^1\text{H}$  NMR (400 MHz, 80 °C,  $\text{C}_2\text{D}_2\text{Cl}_4$ )  $\delta$  = 8.20 (s, 1H), 8.16 (d,  $J$  = 8.2 Hz, 2H), 7.78 (pseudo-d, 4H), 7.74 (d,  $J$  = 8.6 Hz, 2H), 4.61 (m, 2H), 4.58 (m, 2H); IR ( $\text{cm}^{-1}$ ) 1613, 1593, 1511, 1489, 1454, 1432, 1372, 1319, 1239, 1167, 1110, 1096, 1083, 1063, 1014, 977, 963, 890, 836, 819, 759, 696, 623, 592; HRMS ESI-TOF  $m/z$  calculated for  $\text{C}_{26}\text{H}_{15}\text{F}_6\text{N}_2\text{O}_2\text{S}_3$  [M], 597.0194; found, 597.0182.

**5,7-Bis(2-(4-(trifluoromethyl)phenyl)thiazol-5-yl)-2,3-dihydrothieno[3,4-b][1,4]dioxine (12).** Molecular weight 596.59 g/mol; orange solid; mp = 299–300 °C; method A yield 58%;  $^1\text{H}$  NMR (400 MHz, 80 °C,  $\text{C}_2\text{D}_2\text{Cl}_4$ )  $\delta$  = 8.17 (d,  $J$  = 8.2 Hz, 2H), 8.14 (s, 1H), 7.79 (d,  $J$  = 8.3 Hz, 2H), 4.54 (s, 2H); IR ( $\text{cm}^{-1}$ ) 1613, 1594, 1474, 1451, 1425, 1316, 1166, 1108, 1082, 1063, 1015, 984, 972, 851, 826, 776, 759, 635, 627, 590; HRMS ESI-TOF  $m/z$  calculated for  $\text{C}_{26}\text{H}_{15}\text{F}_6\text{N}_2\text{O}_2\text{S}_3$  [M], 597.0194; found, 597.0185.

## ■ ASSOCIATED CONTENT

### ■ Supporting Information

$^1\text{H}$  NMR spectra, X-ray diffraction characterization for trimers 1–3, and density functional theory computational details. Crystallographic information files (CIF) have been deposited with the CCDC with deposition numbers 1009699 and 1009700. This material is available free of charge via the Internet at <http://pubs.acs.org>.

## ■ AUTHOR INFORMATION

### Corresponding Authors

\*E-mail: [patrick.leveque@unistra.fr](mailto:patrick.leveque@unistra.fr).

\*E-mail: [leclercn@unistra.fr](mailto:leclercn@unistra.fr).

### Notes

The authors declare no competing financial interest.

## ■ ACKNOWLEDGMENTS

This work was supported by the French National Research Agency (ANR TANDORI project, ANR-11-PRGE-0011). Nancy Pariona Mendoza is acknowledged for the help with synthesis. Dr. Paul Montgomery is kindly acknowledged for his careful reading of the manuscript.

## ■ REFERENCES

- (1) Breitung, E. M.; Shu, C.-F.; McMahon, R. J. *J. Am. Chem. Soc.* **2000**, *122*, 1154–1160.
- (2) Prasad, P. N.; Williams, D. J. *Introduction to Nonlinear Optical Effects in Molecules and Polymers*; Wiley: New York, 1991.
- (3) Osaka, I.; Zhang, R.; Sauv , G.; Smilgies, D.-M.; Kowalewski, T.; McCullough, R. D. *J. Am. Chem. Soc.* **2009**, *131*, 2521–2529.
- (4) Guo, X.; Quinn, J.; Chen, Z.; Usta, H.; Zheng, Y.; Xia, Y.; Hennek, J. W.; Ortiz, R. P.; Marks, T. J.; Facchetti, A. *J. Am. Chem. Soc.* **2013**, *135*, 1986–1996.
- (5) Le, Y.; Nitani, M.; Karakawa, M.; Tada, H.; Aso, Y. *Adv. Funct. Mater.* **2010**, *20*, 907–913.
- (6) Zaborova, E.; Ch vez, P.; Bechara, R.; L v que, P.; Heiser, T.; M ry, S.; Leclerc, N. *Chem. Commun.* **2013**, *49*, 9938–9940.
- (7) (a) Kuwabara, J.; Yasuda, T.; Choi, S. J.; Lu, W.; Yamazaki, K.; Kagaya, S.; Han, L.; Kanbara, T. *Adv. Funct. Mater.* **2014**, *24*, 3226–3233. (b) Facchetti, A.; Vaccaro, L.; Marrocchi, A. *Angew. Chem., Int. Ed.* **2012**, *51*, 3520–3523.
- (8) Alberico, D.; Scott, M. E.; Lautens, M. *Chem. Rev.* **2007**, *107*, 174–238.
- (9) Lu, W.; Kuwabara, J.; Kanbara, T. *Polym. Chem.* **2012**, *3*, 3217–3219.
- (10) Li gault, B.; Lapointe, D.; Caron, L.; Vlassova, A.; Fagnou, K. *J. Org. Chem.* **2009**, *74*, 1826–1834.
- (11) Liu, X.; Shi, J.-L.; Yan, J.-X.; Wei, J.-B.; Peng, K.; Dai, L.; Li, C.-G.; Wang, B.-Q.; Shi, Z.-J. *Org. Lett.* **2013**, *15*, 5774–5777.

(12) Tani, S.; Uhera, T. N.; Yamaguchi, J.; Itami, K. *Chem. Sci.* **2014**, *5*, 123–135.

(13) Shibahara, F.; Yamaguchi, E.; Murai, T. *J. Org. Chem.* **2011**, *76*, 2680–2693.

(14) Tamba, S.; Okubo, Y.; Tanaka, S.; Monguchi, D.; Mori, A. *J. Org. Chem.* **2010**, *75*, 6998–7001.

(15) Strotman, N. A.; Chobanian, H. R.; Guo, Y.; He, J.; Wilson, J. E. *Org. Lett.* **2010**, *12*, 3578–3581.

(16) Herrmann, W. A.; Brossmer, C.; Reisinger, C.-P.; Riermeier, T. H.;  fele, K.; Beller, M. *Chem.—Eur. J.* **1997**, *3*, 1357–1364.

(17) Berrouard, P.; Najari, A.; Pron, A.; Gendron, D.; Morin, P.-O.; Pouliot, J.-R.; Veilleux, J.; Leclerc, M. *Angew. Chem., Int. Ed.* **2012**, *51*, 2068–2071.

(18) Trimer 1 was already referenced in the CCDC database, under the code KAPWII, prior the beginning of our work. We obtained crystallographic data similar to those reported by growing our own crystals of 1.

(19) Akhtaruzzaman, M.; Tomura, M.; Nishida, J.-I.; Yamashita, Y. *J. Org. Chem.* **2004**, 2953–2958.

(20) (a) Fukazawa, A.; Kishi, D.; Tanaka, Y.; Seki, S.; Yamaguchi, S. *Angew. Chem., Int. Ed.* **2013**, *52*, 12091–12095. (b) Yang, Y. S.; Yasuda, T.; Kakizoe, H.; Mieno, H.; Kino, H.; Tateyama, Y.; Adachi, C. *Chem. Commun.* **2013**, *49*, 6483–6485.

(21) Kim, W.-S.; Kim, H.-J.; Gho, C.-G. *Tetrahedron Lett.* **2002**, *43*, 9015–9017.

(22) Yokooji, A.; Okazawa, T.; Satoh, T.; Miura, M.; Nomura, M. *Tetrahedron* **2003**, *59*, 5685–5689.

(23) See <http://www.wavefun.com/>.

(24) Lee, J. Y.; Song, K. W.; Song, H. J.; Moon, D. K. *Synth. Met.* **2011**, *161*, 2434–2440.

(25) Herrmann, W. A.; Brossmer, C.; Reisinger, C.-P.; Riermeier, T. H.;  fele, K.; Beller, M. *Chem.—Eur. J.* **1997**, *3*, 1357–1364.